HIGH-RESOLUTION MONITORING OF SUSPENDED-SEDIMENT CONCENTRATION AND GRAIN SIZE IN THE COLORADO RIVER USING LASER-DIFFRACTION INSTRUMENTS AND A THREE-FREQUENCY ACOUSTIC SYSTEM

David J. Topping, Research Hydrologist, U.S. Geological Survey, Golden, Colorado, dtopping@usgs.gov; Scott A. Wright, Hydrologist, U.S. Geological Survey, Flagstaff, Arizona, sawright@usgs.gov; Theodore S. Melis, Physical Scientist, U.S. Geological Survey, Flagstaff, Arizona, tmelis@usgs.gov; David M. Rubin, Research Geologist, U.S. Geological Survey, Santa Cruz, California, drubin@usgs.gov

Abstract: In August 2002, we began testing a laser-acoustic system to monitor suspended-sediment transport on the Colorado River in Grand Canyon. This system consists of laser-diffraction, i.e., LISST[1] (Laser In-Situ Scattering and Transmissometry), instruments connected to an automatic pump sampler and an array of three sideways-looking acoustic-Doppler profilers at different frequencies. Stable functions have been developed relating the pump, laser-diffraction, acoustic-attenuation, and acoustic-backscatter measurements to cross-sectionally integrated measurements of suspended-sediment concentration and grain size. We relate acoustic attenuation to the concentration of suspended silt and clay; this approach yields accurate silt and clay concentrations over the range from less than 10 mg/l to about 20,000 mg/l. Suspended-sand concentration can then be computed as functions of the acoustic backscatter and acoustic attenuation; this approach yields accurate sand concentrations over the range from about 10 mg/l to over 3,000 mg/l. LISST-100 and three-frequency-acoustic measurements of the median grain grain size of the suspended sand are typically within 10% of the values of the median grain size measured by conventional methods. Silt and clay loads and sand loads computed by either the LISST-100, LISST-25X, or the three-frequency acoustic system are well within 5% of the values computed using conventional cross-section data (that have errors for silt and clay concentration of ~8% and errors for sand concentration of ~22%). This result, in conjunction with the fact that orders of magnitude more sediment-transport data can be collected each day by the laser-diffraction and acoustic instruments, indicates that a much more complete, and therefore more accurate record of suspended-sediment transport can be collected by the laser-acoustic instruments than by conventional methods alone.

INTRODUCTION

The grain-size distribution of suspended sediment in the regulated Colorado River below Glen Canyon Dam is bimodal, with a silt and clay mode (dominated by clay-sized particles) and a sand mode. Transport of both modes is limited by episodic resupply from tributaries. Transport of the sand mode is regulated by both the discharge of water and short-term changes in the grain size of sand available for transport. During tributary floods, sand on the bed of the river fines; this causes the suspended sand to fine and the suspended-sand concentration to increase, even when the discharge of water remains constant. Subsequently, the bed is winnowed of finer sand, the suspended sand coarsens, and the suspended-sand concentration decreases independently of discharge. This prohibits the computation of sand-transport rates in the Colorado River using stable relations between water discharge and sand transport, and therefore requires a more continuous method for measuring sand transport. To monitor sediment transport in the Colorado River in Grand Canyon, Arizona, we have designed and evaluated a laser-acoustic system for measuring the concentration and grain size of suspended sediment every 15 minutes. Earlier tests of this system were reported in Melis et al. (2003) and Topping et al. (2004).

TEST SITE AND EQUIPMENT

The instrument test site for this study is the Colorado River near Grand Canyon, Arizona, gaging station, hereafter referred to as the Grand Canyon gaging station (Fig. 1). At this test site, the laser-acoustic system consists of: (1) a Sequoia Scientific LISST-100 type C laser-diffraction instrument and a Sequoia Scientific LISST-25X type C laser-diffraction instrument, (2) an ISCO 6712 automatic pump sampler, and (3) three single-frequency Nortek acoustic-Doppler profilers. The ISCO pump sampler is triggered by either of the LISST instruments when laser transmission drops below a user-defined threshold (due to higher suspended-sediment concentrations) and then samples at a user-

[1] Use of brand and firm names in this paper does not constitute endorsement by the U.S. Geological Survey.

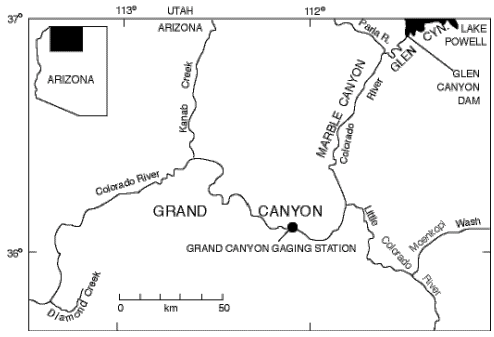

Figure 1 Map of the study area showing the location of the test site at the Colorado River near Grand Canyon, Arizona gaging station, U.S. Geological Survey (USGS) station number 09402500.

defined rate. This allows samples to be collected when the suspended-sediment concentrations exceed the upper sand limit for the LISST and the acoustic-Doppler profilers (around 2,000-3,000 mg/l). The two LISST instruments are suspended in the river from a steel cable on pulleys attached to a vertical cliff (Fig. 2a). The sampling path length of each LISST instrument is 1 cm. The LISST-100 averages 100 samples collected over 30 consecutive seconds out of every 15 minutes; output is volume concentration of suspended sediment in each of 32 log-spaced size classes from 0.0025 to 0.50 mm, water temperature, pressure, and laser transmission. The LISST-25X averages 1000 samples collected over 110 consecutive seconds out of every 15 minutes; output is volume concentration of suspended total sediment (0.0025 to 0.50 mm), volume concentration of suspended sand (0.0625 to 0.50 mm), Sauter mean sizes of suspended total sediment and sand, and laser transmission.

The three-frequency sideways-looking acoustic-Doppler profiler array is mounted on a cart attached to a vertical H-beam bracket anchored to a vertical concrete wall at the base of the gaging station stilling well (Fig. 2a). The cart is stationary at the base of the bracket during periods of data collection, and is raised to the surface (Fig. 2b) only to perform maintenance. The three acoustic-Doppler profilers mounted on this cart are a 1 MHz Nortek EZQ, 2 MHz Nortek EZQ, and a 600 kHz Nortek Aquadopp. These instruments were set to sample 13 out of every 15 minutes in the early phases of our tests; to conserve power, they are now set to sample 10 out of every 15 minutes.

The ISCO 6712 automatic pump sampler (Figs. 2a & 2c) has a capacity of 24 one-liter bottles. We designed the LISST-ISCO pump-sampler control circuit to allow data collection during periods when the river is so greatly enriched with suspended silt and clay that no usable data can be collected by either the LISST or acoustic-Doppler profilers. The protocol is as follows: when the LISST laser transmission is less than the user-defined threshold, the automated program of the ISCO pump sampler is enabled and samples are pumped at pre-defined intervals until either the laser transmission exceeds the user-defined threshold, or the supply of 24 one-liter sample bottles is exhausted.

Data from the laser-acoustic system are downloaded over the internet via a two-way-broadband satellite system installed at the test site. This system was designed by Glenn Bennett and Tim Andrews (USGS, Flagstaff, Arizona) and consists of an on-site computer running the Symantec software "pcAnywhere," a satellite modem, a second computer that boots the system up each morning at a user-defined time for a user-defined duration, and a satellite dish (located on the cliff about 40 m above the gage house in Fig. 2a). The power supplies for the laser-acoustic system and the satellite system consist of 12V deep-cycle batteries (Fig. 2c) recharged by solar panels located on the cliff above the gage house.

DATA USED TO CALIBRATE THE LASER-ACOUSTIC MEASUREMENTS

Computation of cross-sectionally averaged suspended-sediment concentration and grain size from the automatic pump, LISST, and acoustic data was a two-step process. First, the at-a-point pump-measured values of concentration and grain size were calibrated to the corresponding velocity-weighted cross-sectionally averaged values measured at the cableway 200 m downstream (Fig. 2d) using the Equal-Discharge-Increment (EDI) method

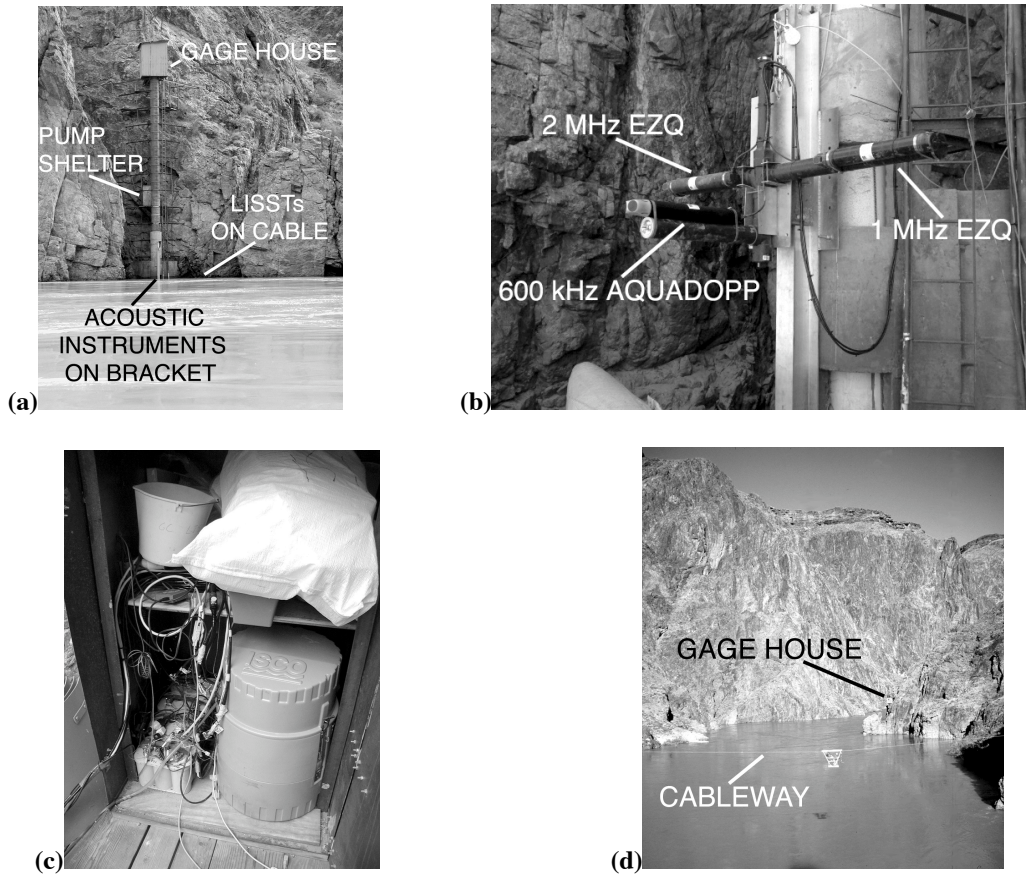

Figure 2 (a) Locations of instrument deployments at Grand Canyon gaging station. (b) Three-frequency acoustic-Doppler profiler array (out of water). (c) Contents of pump shelter in (a) showing automatic pump sampler (on right) and batteries. (d) Upstream view of reach showing measurement cableway and gage house in (a); cableway is 200 m downstream from gage house.

(described in Edwards and Glysson, 1999). The following point values measured with the pump were thus calibrated to the comparable cross-sectionally averaged values from the EDI measurements: the concentration of silt and clay (with $R^2 = 0.997$), the discharge-weighted concentration of total sand (with $R^2 = 0.971$), the discharge-weighted concentration of sand in three size classes [0.0625-0.088 mm (with $R^2 = 0.947$), 0.088-0.177 mm (with $R^2 = 0.967$), and 0.177-1.0 mm (with $R^2 = 0.891$)], and the median grain size of the suspended sand (with $R^2 = 0.826$). Calibration of the pump data for the three size classes of sand was conducted to aid in the calibration of the three single-frequency acoustic-Doppler profilers. This first step in the calibration process used 102 paired EDI and pump samples collected between January 2002 and November 2004 in discharges ranging from 190 to 1,210 m^3/s. Because depth-integrated samplers do not collect time-averaged samples (and therefore do not average over the fluctuating component of the flux due to the turbulent fluctuations in velocity and concentration), the errors associated with EDI measurements are large, i.e., about 8% for silt and clay concentration, 22% for sand concentration, and 12% for the median grain size of the suspended sand (Topping et al., *JGR*, in prep.). Therefore, to ensure that the combination of these large errors with a small sample size (i.e., if only the EDI measurements were used) did not bias the calibrations of the LISST and acoustic measurements, we calibrated the LISST and acoustic measurements to the much larger combined EDI and calibrated-pump dataset.

CALIBRATION OF THE LISST INSTRUMENTS

Calibration of the at-a-point LISST measurements to the "cross-sectionally averaged" (i.e., combined EDI and calibrated-pump) measurements depended primarily on sediment concentration, and secondarily on the discharge of

water (which affects how sediment is mixed between the main flow and the LISST deployment site). The data used for the LISST-100 calibrations were the 443 cross-sectionally averaged measurements made between January 2003 and November 2004; the data used for the LISST-25X calibrations were the 269 cross-sectionally averaged measurements made between June 2003 and November 2004. The LISST-100 and 25X measurements of concentration and grain size were calibrated to the cross-sectionally averaged concentration and grain-size data after segregating the data into five discrete discharge increments: <280 m^3/s, 280-420 m^3/s, 420-570 m^3/s, 570-850 m^3/s, and >850 m^3/s. Equations were then developed to relate the calibrations of suspended-silt and clay concentration, suspended-sand concentration, and suspended-sand median grain size among the five discharge increments. The equations relating the at-a-point silt and clay concentration measured by the LISST-100 and 25X to the cross-sectionally averaged silt and clay concentration were power laws, with exponents that increased non-linearly from 0.55 to 0.74 as a function of increasing discharge (with $R^2 = 0.960$ for the LISST-100 and $R^2 = 0.823$ for the LISST-25X). The equations relating the at-a-point sand concentration measured by the LISST-100 and 25X to the cross-sectionally averaged sand concentration were linear, with coefficients that increased linearly from 0.3 to 3.0 as a function of increasing discharge (with $R^2 = 0.971$ for the LISST-100 and $R^2 = 0.932$ for the LISST-25X). Finally, the equation relating the at-a-point median grain size of the suspended sand measured by the LISST-100 to the cross-sectionally averaged median grain size of the suspended sand was linear, with a coefficient that increased logarithmically from 0.2 to 0.4 as a function of increasing discharge (with $R^2 = 0.937$). No stable relation existed between the Sauter mean diameter of the suspended sand measured by the LISST-25X and either the median grain size of the suspended sand measured by the LISST-100 or the cross-sectionally averaged median grain size of the suspended sand. Therefore, although the LISST-25X accurately measures suspended-sediment concentration in two size classes (i.e, silt and clay, and sand), it does not provide accurate suspended-sand grain-size data at our test site.

CALIBRATION OF THE MEASUREMENTS OF ACOUSTIC ATTENUATION AND ACOUSTIC BACKSCATTER

Theory and measurements of underwater acoustics indicate that, for a given frequency of sound in water, bimodal grain-size distributions of suspended sediment such as those in the Colorado River can be segregated into two acoustic size classes: (1) a finer acoustic size class in which increasing concentration (or decreasing grain size at a constant concentration) results in increased attenuation of sound due to viscous losses (Urick, 1948; Flammer, 1962; Lohrmann, 2001; Gartner, 2004), and (2) a coarser acoustic size class in which increasing concentration (or increasing grain size at a constant concentration) results mainly in increased backscatter of sound (Thorne and Campbell, 1992; Thorne et al., 1993; Lohrmann, 2001; Thorne and Hanes, 2002; Gartner, 2004). At low concentrations of this second acoustic size class (<100 mg/l), concentration is related to backscattered sound pressure (in Pa) increased to the second power, or backscattered sound intensity (in decibels) increased to the fourth power (Thorne and Campbell, 1992; Thorne et al., 1993; Gartner, 2004). At higher concentrations of this second acoustic size class, however, increases in concentration result in increased attenuation of the acoustic energy due to scattering losses (Flammer, 1962; Gartner, 2004), and, at extremely high concentrations (>>1,000 mg/l), result in either no increase or a decrease in the backscattered acoustic energy (Thorne and Campbell, 1992; Thorne et al., 1993). The concentration threshold at which attenuation becomes important in this coarser acoustic size class depends on frequency, with this threshold being lower for higher frequencies of sound (Flammer, 1962). For example, Thorne and Campbell (1992) showed, using a 3 MHz transducer, that attenuation of acoustic energy resulted in substantial deviation from the power of two relation between backscattered sound pressure and sand concentration when the concentration exceeded about 100 mg/l. Power-law curves fit to the theoretically derived relations in Fig. 8 in Thorne and Campbell (1992) have exponents >10 (i.e., all much larger than two) as a result of the increased importance of attenuation relative to backscatter. The threshold grain size between the two acoustic size classes of sediment is negatively correlated with the frequency of sound (Flammer, 1962; Lohrmann, 2001). For a given concentration of sediment, lower frequencies of sound will return proportionately more backscatter from coarser sediment than finer sediment (Thorne and Hanes, 2002, Eqs. 7-10).

The approach employed builds on that in Topping et al. (2004) and takes advantage of the acoustical effects of the two acoustic size classes of sediment to: (1) relate increases in the attenuation of acoustic energy measured by the three single-frequency acoustic-Doppler profilers to increases in silt and clay concentration (this can be accomplished using any one of the three frequencies), (2) for small ranges in this acoustic attenuation due to silt and clay (expressed as a ratio of the acoustic signal strength in a far-field cell to the acoustic signal strength in a near-

field cell), relate increases in the amplitude of the acoustic signal strength to increases in the concentration of either total sand or a specified size class of sand (Fig. 3). The relation between the acoustic attenuation (expressed as this ratio) and silt and clay concentration is linear (Fig. 4a). At lower sand concentrations, the amplitude of the acoustic signal strength in a cell is dominated by backscattered acoustic energy, whereas at higher sand concentrations, the amplitude of the acoustic signal strength results from a combination of backscatter and attenuation. Because of the combined effects of backscatter and attenuation, the relation between the amplitude of the acoustic signal strength and sand concentration is a power law with an exponent that ranges between 10 and 20, depending on frequency and site geometry (Fig. 4b). At a fixed frequency at a given site, this exponent is constant and does not depend on silt and clay concentration. For small ranges in the above-described acoustic-attenuation ratio (arising from suspended silt and clay), a unique power-law relation will exist between the amplitude of the acoustic signal strength in a given cell and the concentration of sand. Thus, a family of power-law curves with identical exponents will exist over a broader range of silt and clay concentration. These curves are related to one another by a coefficient *k* that varies as a function of the acoustic-attenuation ratio. Next, the fact that the threshold grain size between the two acoustic size classes decreases as a function of increasing frequency of sound is used to develop empirical relations between

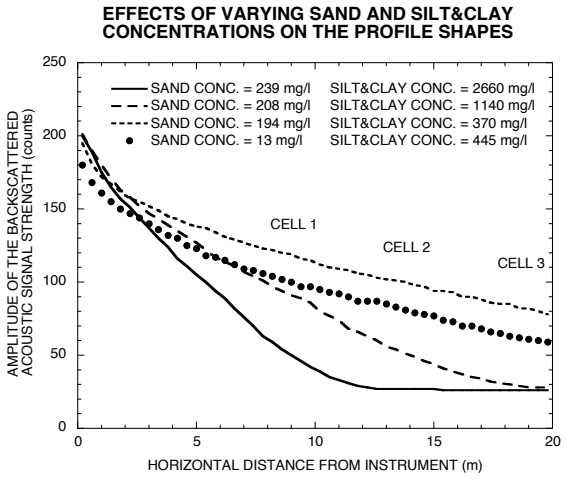

Figure 3 Effects of varying sediment concentration on acoustic profiles collected with the 1 MHz EZQ. Changes in silt and clay concentration mainly result in changes in the slope of the profile; changes in sand concentration mainly result in upward or downward shifts in the profile without changing the slope.

the amplitudes of the acoustic signal strength in a given cell at 600 kHz, 1 MHz, and 2 MHz to the concentration of sand in three size classes. These three size classes of sand were chosen on the basis of the minima in the attenuation-coefficient curves in Flammer (1962, Fig. 1) and are the same as those used above in the calibration of the pump data to the EDI measurements: 0.0625-0.088 mm, 0.088-0.177 mm, and 0.177-1.0 mm. Finally, logarithmic interpolation between the acoustically computed sand concentration in each size class is used to compute an "acoustic median grain size" (i.e., acoustic D_{50}) for the suspended sand.

The standard method for working with acoustic-attenuation and backscatter data is to convert the measured amplitudes of the signal strength in each cell (in counts) to sound intensity (in decibels) using the sonar equation of Urick (1975). This equation takes into account the two-way transmission losses due to beam spreading, the attenuation due to absorption by the water (which depends on pressure, temperature, and salinity), and the attenuation due to viscous or scattering losses by the suspended sediment. Because all of these terms are linear, and the pressure, temperature, and salinity do not vary greatly at the Grand Canyon gaging station test site, one does not gain much in the analysis by converting to sound intensity and using the sonar equation (besides determining that the values of the attenuation due to the suspended sediment fall in the normal range of about 0 to 20 dB/m). In the examples below, therefore, measured raw amplitudes in the acoustic signal strength (in counts) are used to compute the acoustic attenuation in terms of a ratio of counts in a far-field cell to counts in a near-field cell (Figs. 3 & 4).

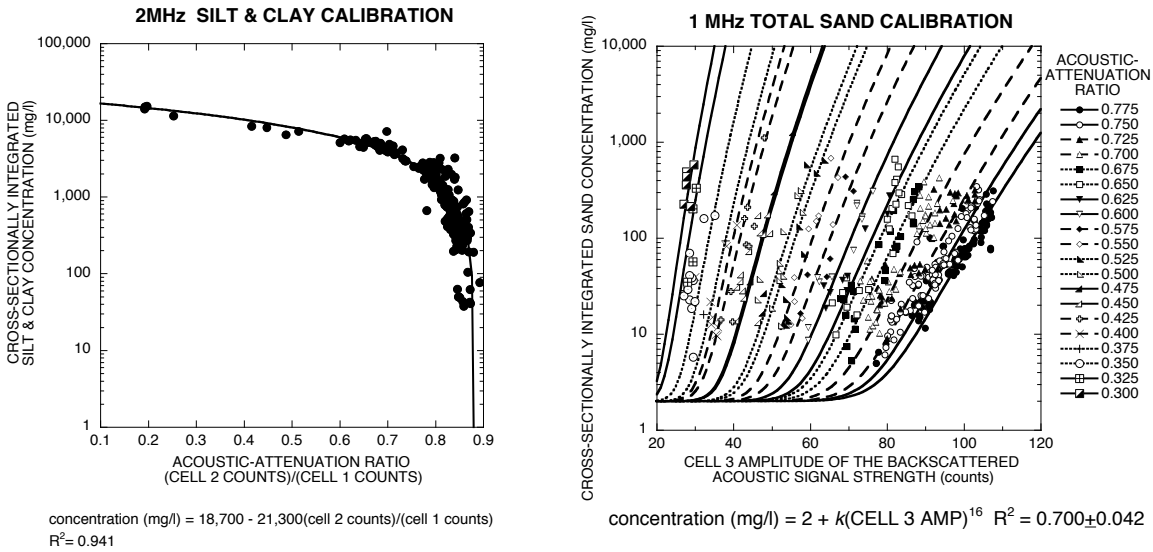

(a) **(b)**

Figure 4 (a) Example of the relation between acoustic attenuation at 2 MHz (expressed as a ratio in counts between cells) and silt and clay concentration. (b) Example of the relations between the amplitude of the acoustic signal strength measured by the 1 MHz EZQ and total sand concentration for small ranges in the acoustic-attenuation ratio arising from silt and clay. The coefficient k relates the sand-calibration curves as a function of the acoustic attenuation ratio, i.e., silt and clay concentration (relation has $R^2 = 0.986$).

RESULTS

The laser-acoustic measurements are in excellent agreement with the EDI and calibrated pump measurements. The levels of agreement between the integrated loads (computed by summing the instantaneous loads) and integrated grain size are shown in Table 1. For comparison, errors associated with the EDI measurements against which the

Table 1 Difference in the integrated laser-acoustic measurements relative to the integrated combined EDI, calibrated pump measurements (using both calibrated and uncalibrated laser-acoustic data).

	LISST-100	LISST-25X	1 MHz only	3-frequency
Silt and clay load	+5.0%	-0.5%	-2%	-2%
Total sand load	+0.4%	+1.0%	-4%	-3%
0.0625-0.088 mm sand load	Not analyzed	N/A	N/A	-10%
0.088-0.177 mm sand load	Not analyzed	N/A	N/A	-4%
0.177-1.0 mm sand load	Not analyzed	N/A	N/A	-1%
Suspended-sand D_{50}	+0.5%	N/A	N/A	+4.8%

laser-acoustic measurements were calibrated are much larger than the values in Table 1: ~8% for silt and clay concentration, ~22% for sand concentration, and ~12% for suspended-sand median grain size. Comparison of laser-acoustic, pump, and cableway measurements of silt and clay concentration, sand concentration, and suspended-sand median grain size beyond the calibration period ending in November 2004 are shown in Fig. 5. As shown in Fig. 5, the calibrations for concentration and grain size are stable for the pump, LISST, and acoustic measurements and the agreement remains excellent beyond the period used for calibration. Therefore, because of the larger errors associated with the EDI measurements, the stability of the laser-acoustic calibrations, and the fact that orders of magnitude more sediment-transport data can be collected each day by the laser-diffraction and acoustic instruments, a much more complete, and therefore more accurate record of suspended-sediment transport can be collected by the laser-acoustic instruments than by conventional methods alone.

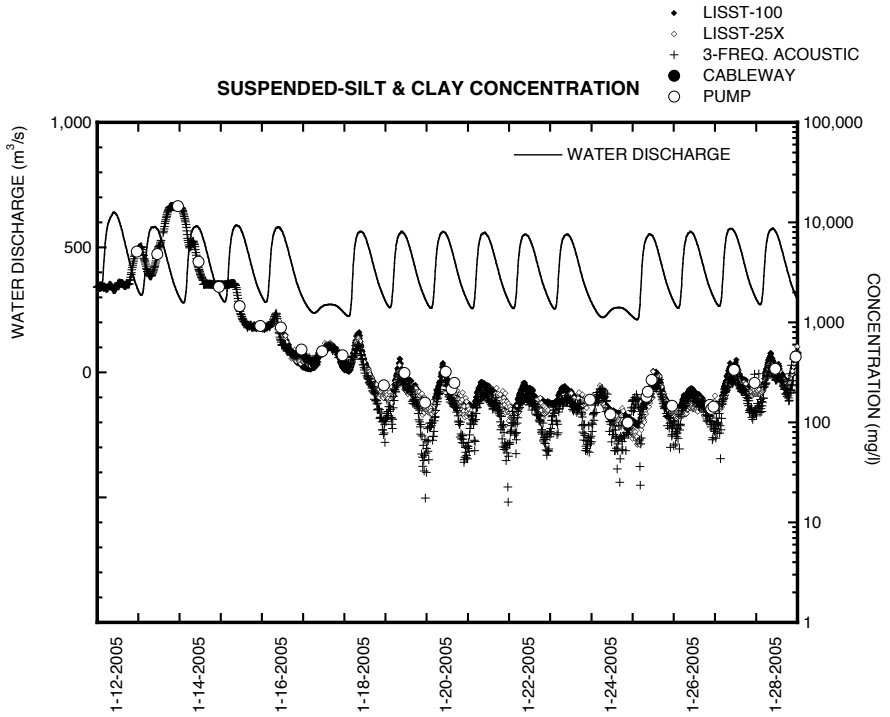

(a)

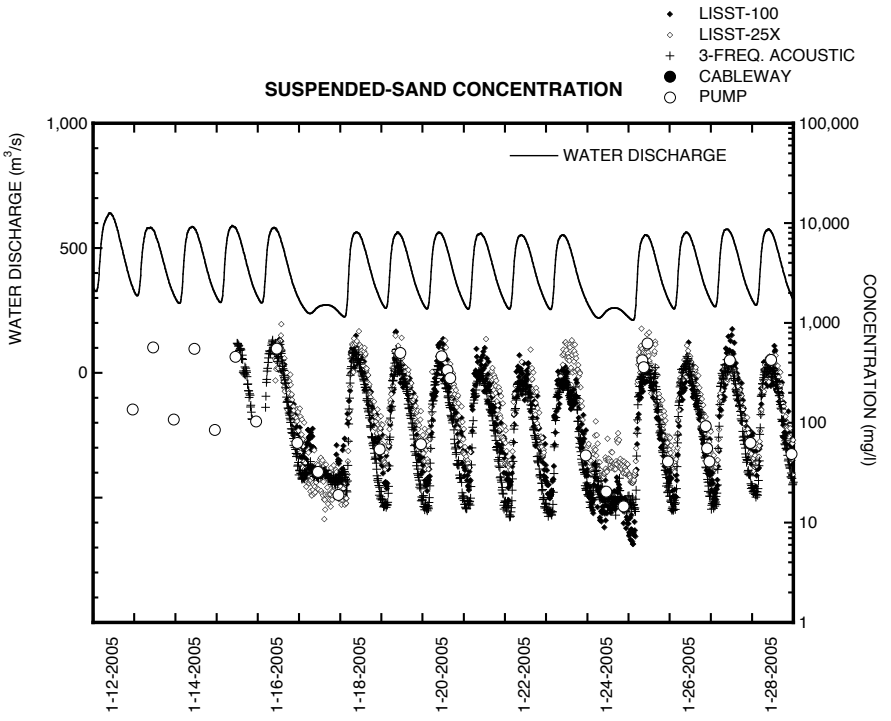

(b)

Figure 5 Examples of the high-resolution laser-acoustic suspended-sediment data from beyond the period of calibration. No EDI measurements were made from the cableway during this 17-day period. Silt and clay concentrations were too high during the first 3 1/2 days of this period to get LISST or acoustic measurements of suspended-sand concentration or median grain size. (a) Silt and clay concentration, (b) Sand concentration, (c) Suspended-sand median grain size (D_{50}); on next page.

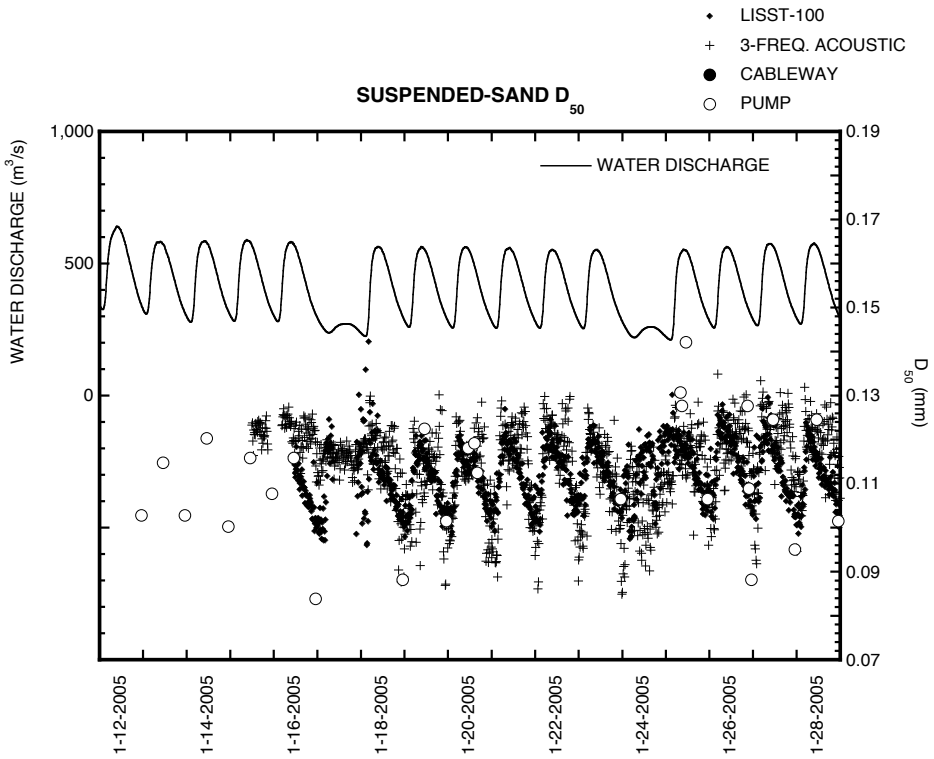

Figure 5 **(c)**

REFERENCES

Edwards, T.K., and Glysson, G.D., 1999, Field methods for measurement of fluvial sediment: *U.S. Geological Survey Techniques of Water-Resources Investigations Book 3, Chap. C2*, 89p.

Flammer, G.H., 1962, Ultrasonic measurement of suspended sediment: *U.S. Geological Survey Bulletin 1141-A*, 48 p.

Gartner, J.W., 2004, Estimating suspended solids concentrations from backscatter intensity measured by acoustic Doppler current profiler in San Francisco Bay, California: *Marine Geology*, v. 211, p. 169-187.

Lohrmann, A., 2001 Monitoring sediment concentration with acoustic backscattering instruments: *Nortek Technical Note No. 3*, 5 p., downloadable from http://www.nortek-as.com/.

Melis, T.S., Topping, D.J., and Rubin D.M., 2003, Testing laser-based sensors for continuous in situ monitoring of suspended sediment in the Colorado River, Arizona, *in* Bogen, J., Fergus, T., and Walling, D.E., eds., Erosion and Sediment Transport Measurement in Rivers: Technological and Methodological Advances: Wallingford, Oxfordshire, United Kingdom, IAHS Press, IAHS Publication 283, p. 21-27.

Thorne, P.D., and Campbell, S.C., 1992, Backscattering by a suspension of spheres: *Journal of the Acoustical Society of America*, v. 92, n. 2, p. 978-986.

Thorne, P.D., Hardcastle, P.J., and Soulsby, R.L., 1993, Analysis of acoustic measurements of suspended sediments: *Journal of Geophysical Research*, v. 98, n. C1, p. 899-910.

Thorne, P.D., and Hanes, D.M., 2002, A review of acoustic measurements of small-scale sediment processes: *Continental Shelf Research*, v. 22, p. 603-632.

Topping, D.J., Melis, T.S., Rubin, D.M., and Wright, S.A., 2004, High-resolution monitoring of suspended-sediment concentration and grain size in the Colorado River in Grand Canyon using a laser-acoustic system, *in* Hu, C., and Tan, Y, eds., Proceedings of the Ninth International Symposium on River Sedimentation, October 18-21, 2004, Yichang, China: People's Republic of China, Tsinghua University Press, p. 2507-2514.

Urick, R.J., 1948, The absorption of sound in suspension of irregular particles: *Journal of the Acoustical Society of America*, v. 20, n. 3, p. 283-289.

Urick, R.J., 1975, Principles of Underwater Sound for Engineers: New York, McGraw Hill, 384 p.